Science of the Total Environment 714 (2020) 136693

Contents lists available at ScienceDirect

Science of the Total Environment

journal homepage: www.elsevier.com/locate/scitotenv

Spatio-temporal variability of desert dust storms in Eastern Mediterranean (Crete, Cyprus, Israel) between 2006 and 2017 using a uniform methodology

Souzana Achilleos [a,*], Petros Mouzourides [b], Nikos Kalivitis [c,d], Itzhak Katra [e], Itai Kloog [e], Panayiotis Kouis [f], Nicos Middleton [g], Nikos Mihalopoulos [c,d], Marina Neophytou [b], Andrie Panayiotou [a], Stefania Papatheodorou [a,h], Chrysanthos Savvides [i], Filippos Tymvios [j,k], Emily Vasiliadou [i], Panayiotis Yiallouros [f,1], Petros Koutrakis [l,1]

[a] Cyprus International Institute for Environmental and Public Health, Cyprus University of Technology, Cyprus
[b] Department of Civil and Environmental Engineering, University of Cyprus, Cyprus
[c] Department of Chemistry, University of Crete, Greece
[d] National Observatory of Athens, Greece
[e] Department of Geography and Environmental Development, Ben-Gurion University of the Negev, Israel
[f] Medical School, Cyprus University, Cyprus
[g] Department of Nursing, Cyprus University of Technology, Cyprus
[h] Department of Epidemiology, Harvard T.H. Chan School of Public Health, USA
[i] Department of Labour Inspection, Ministry of Labour, Welfare and Social Insurance, Cyprus
[j] Cyprus Department of Meteorology, Cyprus
[k] The Cyprus Institute, Cyprus
[l] Department of Environmental Health, Harvard T.H. Chan School of Public Health, USA

HIGHLIGHTS

- Ground and satellite measurements were used to build a dust classification model.
- PM_{10} and dust-AOD were significant indicators for dust identification.
- A higher 24-hr PM_{10} threshold for dust days was found for Israel.
- A steady trend with sporadic peaks was observed for dust characteristics (2006–17).

GRAPHICAL ABSTRACT

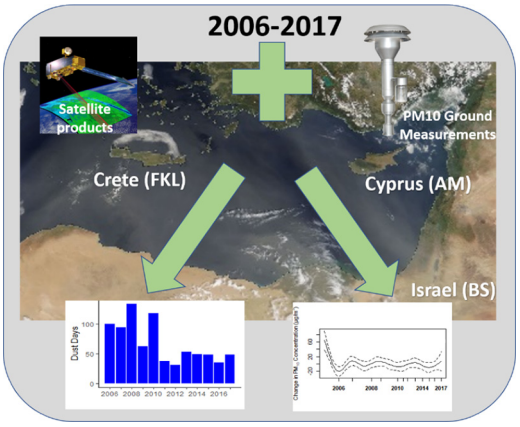

ARTICLE INFO

Article history:
Received 22 October 2019

ABSTRACT

The characteristics of desert dust storms (DDS) have been shown to change in response to climate change and land use. There is limited information on the frequency and intensity of DDS over the last decade at a regional

* Corresponding author.
E-mail address: Souzana.achilleos@cut.ac.cy (S. Achilleos).
[1] Equal senior authorship.

https://doi.org/10.1016/j.scitotenv.2020.136693

Received in revised form 24 December 2019
Accepted 13 January 2020
Available online 15 January 2020

Editor: Pavlos Kassomenos

Keywords:
Dust storms
Trend
PM_{10}
AOD
MENA region

scale in the Eastern Mediterranean. An algorithm based on daily ground measurements (PM_{10}, particulate matter ≤10 μm), satellite products (dust aerosol optical depth) and meteorological parameters, was used to identify dust intrusions for three Eastern Mediterranean locations (Crete-Greece, Cyprus, and Israel) between 2006 and 2017. Days with 24-hr average PM_{10} concentration above ~30 μg/m^3 were found to be a significant indicator of DDS for the background sites of Cyprus and Crete. Higher thresholds were found for Israel depending on the season (fall and spring: PM_{10} > 70 μg/m^3, winter and summer: PM_{10} > 90 μg/m^3).

We observed a high variability in the frequency and intensity of DDS during the last decade, characterized by a steady trend with sporadic peaks. The years with the highest DDS frequency were not necessarily the years with the most intense episodes. Specifically, the highest dust frequency was observed in 2010 at all three locations, but the highest annual median dust-PM_{10} level was observed in 2012 in Crete (55.8 μg/m^3) and Israel (137.4 μg/m^3), and in 2010 in Cyprus (45.3 μg/m^3). Crete and Cyprus experienced the same most intense event in 2006, with 24 h-PM_{10} average of 705.7 μg/m^3 and 1254.6 μg/m^3, respectively, which originated from Sahara desert. The highest 24 h-PM10 average concentration for Israel was observed in 2010 (3210.9 μg/m^3) during a three-day Saharan dust episode. However, a sub-analysis for Cyprus (years 2000–2017) suggests a change in DDS seasonality pattern, intensity, and desert of origin. For more robust conclusions on DDS trends in relation to climate change, future work needs to study data over several decades from different locations.

1. Introduction

Desert dust storms (DDS) are naturally occurring events that transport dust particles far from their sources. During DDS events, which can last from few hours to several days, PM_{10} (particulate matter with aerodynamic diameter ≤ 10 μm) levels are considerably higher than the 2005 EU daily limit value of 50 μg/m^3 (Achilleos et al., 2014; Mouzourides et al., 2015). Daily PM_{10} levels during DDS events can exceed 2000 μg/m^3 (Krasnov et al., 2014). DDS pose a major risk to populations residing in affected areas such as in Mediterranean countries (Querol et al., 2009) situated at the margins of the global dust belt, known as MENA (Middle East and North Africa) region, extending from West Africa to the Arabian Peninsula. Several studies have associated DDS events with increase in daily mortality and hospital admissions (Middleton et al., 2008; Neophytou et al., 2013; Vodonos et al., 2014; Achilleos et al., 2019). The characteristics of DDS have been shown to change both in terms of frequency as well as intensity, in response to climate change and land use; therefore, their health implications are expected to become more severe (Goudie, 2014; Krasnov et al., 2016a). Previous studies have suggested that the frequency of DDS in the southeastern Mediterranean has increased over the last decades (Ganor et al., 2010). In Cyprus, the number of DDS days during the period 1998–2008 increased at an average rate of 1.7 days/year, reaching a peak of 30 DDS days in 2008 (Achilleos et al., 2014). In Crete, during the winter and spring in 2004–2005, background PM_{10} levels exceeded the daily EU limit in 1 out of 5 days, with 80–100% of the incidents linked to DDS (Gerasopoulos et al., 2006). In data from a more recent study period, Krasnov et al. (2016a) showed an increasing trend in daily and hourly PM_{10} levels during DDS events in the Negev region from 2009 up to 2015. However, in previous studies there was no uniform methodology for analysis of DDS frequency and intensity of long-term ground measurements obtained from different sites in the region of the Eastern Mediterranean. In particular, DDS events definition differed considerably in various studies from different sites in the region in the past.

We aimed to apply the same methodology to identify DDS and evaluate their frequency trends and impact on PM levels at three locations in the Eastern Mediterranean: i) Crete-Greece, which is impacted by long range transport commonly from Africa (Kalivitis et al., 2007); ii) Cyprus, impacted by long range transport from both Africa and Middle East (Pikridas et al., 2018); and iii) Israel, impacted by abating deserts of the Arabian Peninsula and long range transport from Africa (Krasnov et al., 2016b).

2. Material and methods

2.1. Study area

We used data obtained at three Eastern Mediterranean monitoring stations located: i) at the Island of Crete, Greece (Finokalia background station; 35°20′ N, 25°40′ E; 250 m asl); ii) in Cyprus (Ayia Marina Xyliatos Nicosia background station; 35°02′ N, 33°03′ E; 532 m asl), and; iii) in Israel (Beer Sheva urban station; 31°15′ N, 34°47′ E) (Fig. 1).

Finokalia (FKL) is the atmospheric research station of the Environmental Chemical Processes Laboratory at the University of Crete, and is located 50 km east of Heraklion, the largest city of the island (population: 173,993; 2011 Census). The area is characterized by a dry season (April to September), a wet season (from October to April), and a Sahara dust season during spring (South/South-West winds; occurrence up to 20% of the days) (Gerasopoulos et al., 2006). The Ayia Marina (AM) station is part of the air quality monitoring network operated by the Air Quality Section, Cyprus Department of Labor Inspection. The monitoring site is located in the Nicosia district, 40 km southwest of the city (population: 332,200; 2011 Census). Cyprus has a Mediterranean climate with hot and dry summers (May–September), and mild winters (November–March). During summer the eastern Mediterranean basin is influenced by a surface trough extending westward from the Levantine, which can be conceived as the westerly extension of the seasonal thermal low induced by the South Asian monsoon that can reach the eastern Mediterranean (Michaelides et al., 1999). It is highly affected by dust transport from both the Saharan and Arabian deserts and DDS usually occur at the end of the winter and during spring (February–May) (Pikridas et al., 2018). Both FKL and AM stations are participating in the network of Co-operative Program for Monitoring and Evaluation of the Long-range Transmission of Air Pollutants in Europe (EMEP).

The city of Beer Sheva (BS), located at the edge of the Negev desert, is one of the main urban areas in Israel (population: 205,810; 2016 Census). BS monitoring station is located on the roof of a building at the city center and it is part of the National Air Monitoring Network, operated by the Israel Ministry of Environmental Protection. Beer Sheva has hot and dry summers, and cool and wet winters. DDS originate from both the Saharan and Arabian region, occurring mostly during the winter and spring (Krasnov et al., 2014).

Fig. 1. Location of the three monitoring sites in Crete-Greece (Finokalia), Cyprus (Ayia Marina Xyliatou), and Israel (Beer Sheva).

2.2. Data

2.2.1. Ground observations

Continuous PM_{10} data for the period 2006–2017 were available from each monitoring station. PM_{10} concentrations were recorded every 5 min using a Tapered Element Oscillating Microbalance (TEOM) (BS) and FH 62 I-R Thermo (FKL) instruments, and every 2 min in AM using TEOM. Hourly measurements of meteorological parameters (temperature, relative humidity, wind speed) were also collected at the monitoring stations. $PM_{2.5}$ and precipitation data were also available from AM and BS stations. Daily averages were calculated for days with at least 12 h of hourly measurements. Daily missing PM_{10} data were replaced, if possible, by gravimetric measurements (AM: $PM_{10\text{-TEOM}} = 1.32 + 0.98\ PM_{10\text{-grav}}$, $R^2 = 0.83$; FKL: $PM_{10\text{-THERMO}} = 0.45 + 0.97\ PM_{10\text{-grav}}$, $R^2 = 0.99$) or, for BS, by regressing $PM_{2.5}$ data from nearby station (Arad-BS) using the following model ($R^2 = 81\%$):

$$PM_{10,i} = \beta_0 + PM_{2.5-Arad,i} + WS_i + Temp_i \quad (1)$$

where, $PM_{10,i}$ is the 24 h-mean PM_{10} concentration for day i; β_0 is the regression intercept; $PM_{2.5\text{-}Arad,i}$ is the 24 h-mean $PM_{2.5}$ from the nearby Arad station for day i; WS_i is the 24 h-mean wind speed from Beer-Sheva station for day i; and $Temp_i$ is the 24 h-mean temperature from Beer-Sheva station for day i.

The remaining missing PM_{10} data for all years were below 20% (AM: 1%, FKL: 16%, BS: 15%). For FKL, in years before 2009 there was a significant percentage of missing PM_{10} data (2006: 29%, 2007: 69%, 2008: 34%); and for BS, this was also the case for years 2011 (40%) and 2012 (69%) (Table S1).

2.2.2. Satellite observations

We obtained 3-hourly aerosol optical depth dust at 550 nm (Dust-AOD_{550}) data from the Copernicus Atmosphere Monitoring Service (CAMS) global reanalysis dataset produced by the European Centre for Medium-Range Weather Forecasts (ECMWF) (Inness et al., 2019). The spatial resolution of the data is approximately 80 km (0.7° × 0.7° grid) and it was available for all three sites (100% complete data). Daily averages were also calculated.

2.3. Data analyses

2.3.1. DDS classification

We followed a DDS classification methodology similar to the one described in Sorek-Hamer et al. (2013), in order to build a classification model for DDS identification. We used both ground and satellite measurements to include both the events where dust was travelling in the lower atmosphere levels but also in the upper levels. Specifically, we followed the steps below:

a) For all three sites, we carefully analyzed a complete two-year (AM and FKL: 2011, 2014; BS: 2011, 2017) dataset. This included daily PM_{10} concentrations, Dust-AOD values, and the corrected reflectance images of the MODIS – Terra and Aqua satellites – from the NASA Worldview application operated by the NASA/Goddard Space Flight Center Earth Science Data and Information System (ESDIS) project (https://worldview.earthdata.nasa.gov/). In addition, we used the daily PM_{10}-to-$PM_{2.5}$ ratio, available for AM and BS; and PM_{10} elemental concentrations available for AM (calcium-Ca, aluminum-Al, iron-Fe) and FKL (Ca).
used as 'reference years' and were selected based on data availability (PM_{10}, Dust-AOD, $PM_{2.5}$, elemental concentrations) and the fact that, after looking at the annual average and daily maximum of PM_{10} concentrations, there was no record of extreme DDS events with PM_{10} concentrations higher than 200 $\mu g/m^3$. The rationale behind this selection was to ensure the sensitivity of our methodology and identify even mild events.
the two reference years, and classified days as DDS (DDS, dust = 1) and non-DDS (NDDS, dust = 0) the days for which we identified peaks in the daily PM_{10} concentrations or Dust-AOD values, and satellite images were indicating suspension of dust around the areas; and, when available, high PM_{10}-to-$PM_{2.5}$ ratio and high crustal elemental concentrations. Based on these criteria, we identified 106 DDS days for AM, 88 DDS for FKL, and 101 DDS for BS during the two reference years.
b) Then, we applied the Classification and Regression Tree (CART) algorithm on the classified days of the reference years which included daily PM_{10} levels, Dust-AOD, meteorological variables (temperature, relative humidity, wind speed), and a categorical variable for season (dataset A), in order to find the best explanatory rules that

distinguishes DDS and NDDS. These variables were chosen to be examined in the CART analysis because they have shown distinct differences between DDS and NDDS (Table S2), and at the same time were available for all three sites. The classification tree model with the smallest cross-validation error identified a set of explanatory factors ("rules") associated with DDS. The rules were then used to transform dataset A to a binary dataset (dataset B). The algorithm was applied for each site separately, using the 'rpart' package in 'R' statistical software (R Core Team, 2018).

c) In order to identify DDS for the rest of the years, we aimed to estimate a cut off value/threshold and a daily probability (output of a Logistic regression model) using the reference years. When the probability for each day was greater than the threshold then that day was marked as a DDS (dust = 1) otherwise it was marked as NDDS (dust = 0). For this reason, we modeled the probability of DDS using a logistic regression model, as:

$$\text{Logit}\,(P) = \ln\left(\frac{P}{1-P}\right) = \beta_0 + \beta_1\, x_1 + \beta_2\, x_2 + \ldots. + \beta_i\, x_i \qquad (2)$$

where, P is the probability of DDS occurrence, β_0 the intercept, β_i the coefficients of the rules x_i obtained from CART. The logistic regression model was applied on a training subset of dataset B (80% of the dataset), and the evaluation was performed on the testing subset (remaining 20% of dataset B). This procedure was repeated 10 times, for 10 different random selections of training and testing datasets. From each run, we estimated and plotted the true positive rate (sensitivity: true DDS were correctly classified as DDS) on the y-axis against the false positive rate (1-specificity: true NDDS were incorrectly classified as DDS) on the x-axis, and produced the Receiver Operator Characteristic Curves (ROC). The threshold value was determined from the ROC curve based on two criteria; point on curve closest to the (0, 1) and Youden index (point that maximizes the sum of sensitivity and specificity, where specificity is the true negative rate and represents the rate of true NDDS correctly classified as NDDS). From the 10 runs, we used the regression coefficients that gave the highest accuracy with the testing dataset (accuracy = 95%) (Table S3). The optimal thresholds were determined based on the average ROC curve (Figs. S1, S2) for each site as: i) AM-optimal threshold = 0.06–0.82 (sensitivity = 0.75, specificity = 0.88, average-AUC = 0.85), ii) FKL-optimal threshold = 0.05–0.39 (sensitivity = 0.72, specificity = 0.88, average-AUC = 0.84), and iii) BS-optimal threshold = 0.07–0.72 (sensitivity = 0.66, specificity = 0.89, average-AUC = 0.79). The combination of CART-regression method identified 89 DDS, 71 DDS, and 68 DDS for AM, FKL, and BS, respectively, when applied for the reference years. For AM and FKL, 73% of DDS and 98% of NDDS were correctly classified, and for BS 69% of DDS and 99% of NDDS were correctly classified.

d) For the final step of DDS classification, we applied the combined CART-regression scheme to all the days of the 12-year study period and classified days as DDS and NDDS. For days with missing data (mainly PM_{10}), we inspected the days in a similar way with the reference years, and identified DDS based on Dust AOD, satellite images, and meteorological variables, PM_{10}-to-$PM_{2.5}$ ratio, PM_{10} elemental concentrations, if were available.

e) In addition, DDS were classified based on their source of origin (Saharan, Middle Eastern-ME, mixture of Saharan and ME deserts) after examining 5-day backward air trajectories traced at 500, 1500 and 2500 m height AGL using the Hybrid Single-Particle Lagrangian Integrated Trajectory (HYSPLIT) model (Stein et al., 2015; Rolph et al., 2017).

2.3.2. Trends analysis

We applied the Theil-Sen estimator and Mann-Kendall test of significance (a nonparametric method to test and model trends) to assess the linear trend of DDS. We also examined the nonlinear trend of PM_{10} concentrations and Dust-AOD during dust days using a Generalized Additive Model (GAM) with a penalized regression spline function on time (DDS date).

$$\mu_i = \beta_0 + f_i\,(\text{DDS}_i) \qquad (3)$$

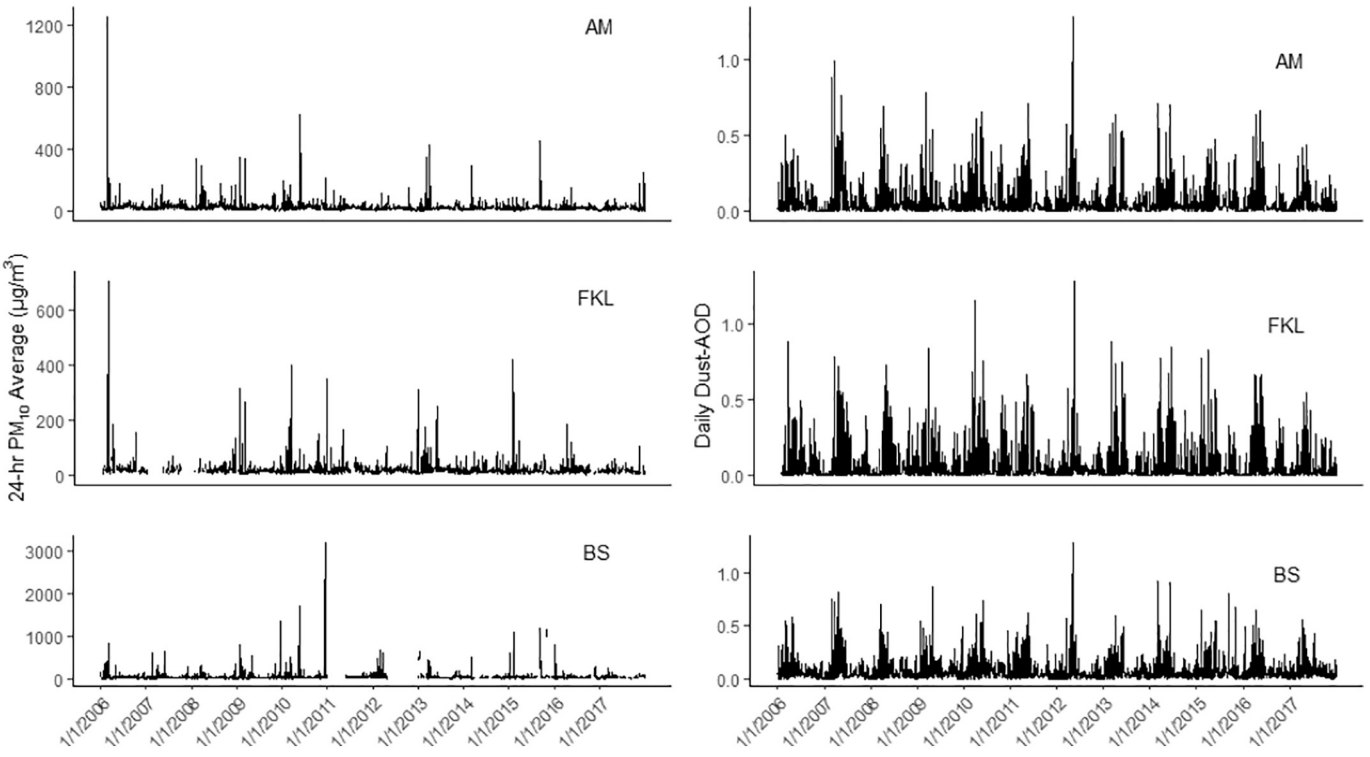

Fig. 2. Average daily concentration of PM_{10} (µg/m^3) and Dust-AOD over the 12-year study period in AM, FKL, and BS.

Table 1
CART classification 'rules' for DDS.

	Rule 1 (x_1)	Rule 2 (x_2)	Rule 3 (x_3)
AM	$PM_{10} \geq 34.7$	$25.0 < PM_{10} < 34.7$ Dust-AOD ≥ 0.12	
FKL	Dust-AOD ≥ 0.15 $PM_{10} \geq 27.6$	Dust-AOD ≥ 0.15 $18.8 \leq PM_{10} < 27.6$ Temperature ≥ 21.9	Dust-AOD < 0.15 $PM_{10} \geq 39.1$
BS	$PM_{10} \geq 66.7$ Season[a]: fall, spring	$PM_{10} \geq 88.4$ Season[a]: summer, winter	$PM_{10} < 66.7$ Dust-AOD ≥ 0.14 Wind speed > 3.1

[a] fall: September–November, winter: December–February, spring: March–May, summer: June–August.

where μ_i is the mean daily PM_{10} concentration or Dust-AOD for DDS day i; β_0 is the regression intercept; and f() represents a penalized regression spline function where the degrees of freedom were determined by choosing the smoothing parameter by Generalized Cross Validation criterion (GCV).

For the trend analyses, we used the 'trend', 'Kendall', "splines", and "mgcv" packages in R statistical software (R Core Team, 2018).

3. Results and discussion

3.1. DDS characteristics

The daily PM_{10} concentration and Dust-AOD time series over the study period 2006–2017 are presented in Fig. 2, and the hourly PM_{10} levels are illustrated in Fig. S3. The daily average PM_{10} values ranged from 2.4 to 1254.6 μg/m^3 in AM; from 2.0 to 705.7 μg/m^3 in FKL; and from 5.2 to 3210.9 μg/m^3 in BS. Dust-AOD was within the range of 0.00 and 1.28 at all sites.

The CART analysis identified two classification rules for AM, and three for FKL and BS. The rules are described in Table 1. Dust-AOD and PM_{10} were the most significant variables in classifying DDS for all three sites. Different DDS criteria (visibility, AOD, aerosol scattering, angstrom exponent, dust aerosol maps, wind direction, synoptic patterns, etc.) have been previously used in several studies (Michaelides et al., 1999; Ganor et al., 2009; Ealo et al., 2016; Chudnovsky et al., 2017; Diapouli et al., 2017; Flores et al., 2017; Michaelides et al., 2017). However, the use of criteria based on ground and columnar aerosol load, and their combination, has been shown to be a reliable tool for DDS classification, since it allows the identification of low, medium, and high intensity events (Kalivitis et al., 2007; Cachorro et al., 2016). Other explanatory variables were temperature for FKL, and wind speed and seasonality for BS. These rules, along with the regression coefficients (Table S2), were used to identify DDS for all years of the study period.

We identified 810 (AM), 451 (FKL) and 633 (BS) DDS in the Eastern Mediterranean region during the twelve-year study period. The majority (85%) of the identified DDS from AM station were described by daily PM_{10} average greater or equal to 34.7 μg/m^3 (AM-CART-rule 1), and almost half (49%) of the FKL DDS were described by daily Dust-AOD average greater or equal to 0.15 and PM_{10} average equal/above 27.6 μg/m^3 (FKL-CART-rule 1). Similarly, in BS, ~60% of the DDS were identified during fall and spring months with PM_{10} average greater or equal to 66.7 μg/m^3 (BS-CART-rule 1), and 26% during winter and summer months with PM_{10} average greater or equal to 88.4 μg/m^3 (BS-CART-rule 2). These percentages also depict the number of DDS that were observed at ground level and affect human health. The rest (15%, 51%, and 14% for AM, FKL, and BS, respectively) represent DDS which occurred at higher atmospheric levels.

Table 2 presents summary statistics for PM_{10} levels, Dust-AOD, and meteorology at the three sites. PM_{10} concentration and Dust-AOD were much higher in BS than in AM and FKL. BS station is set within the city as opposed to the other two stations, which are located in rural areas. Nevertheless, Beer Sheva is a city not impacted by heavy traffic or industry. It is surrounded by large arid areas and as result, the contribution of anthropogenic sources to PM_{10}, even in non-dust days, is only ~15% (Krasnov et al., 2016b).

The three East Mediterranean sites experienced 91 common DDS (AM-PM_{10}:81.7 ± 73.9 μg/m^3, FKL-PM_{10}:62.2 ± 44.6 μg/m^3, BS-PM_{10}:157.1 ± 186.3 μg/m^3), which corresponds to 11% of DDS for AM, 20% for FKL, and 14% for BS. Most of these DDS originated from Saharan desert (n-AM:65, n-FKL:88, n-BS:50) with BS been impacted most intensely (AM-PM_{10}:79.7 ± 77.1 μg/m^3, FKL-PM_{10}:77.6 ± 55.8 μg/m^3, BS-PM_{10}:108.6 ± 88.3 μg/m^3). The rest of the common dust days were influenced from either ME desert (n-AM:18, n-FKL:2, n-BS:21) or from both Saharan and ME deserts (n-AM:8, n-FKL:1, n-BS:20). In addition, AM and BS experienced another 310 common dust days (38% of DDS for AM with PM_{10}:72.3 ± 68.1 μg/m^3, 49% of DDS for BS with PM_{10}:152.8 ± 176.8 μg/m^3), FKL and BS 127 (28% of DDS for FKL with PM_{10}: 58.9 ± 40.2 μg/m^3, 20% of DDS for BS with PM_{10}: 138.0 ± 161.4 μg/m^3), and AM and FKL 188 common dust days (23% of DDS for AM with PM_{10}:70.4 ± 104.3 μg/m^3, 42% of DDS for FKL with PM_{10}:63.3 ± 53.3 μg/m^3).

3.2. Meteorological conditions

FKL had the highest daily average of relative humidity and wind speed, but lowest temperature (Table 2). BS, although is surrounded by large deserts, experienced more precipitation than AM. During DDS, the mean PM_{10} level was up to three (AM, FKL) or five (BS) times higher than the non-dust days average. A four to fivefold increase was observed for Dust-AOD during DDS as well. DDS were associated with higher temperatures and drier conditions at all three sites. DDS were windier in BS, but the opposite was observed in FKL.

The origin of the major PM_{10} sources for the whole study period was studied using the bivariate polar plots for each site (Fig. 3). Bivariate polar plots statistically represent the PM_{10} concentrations in polar coordinates taking into account the wind speed and direction. Two different versions of the plots are shown; Fig. 3a–d show how the PM_{10} concentrations vary per season depending on local wind speed and direction and; therefore, the direction of high PM_{10} concentrations (red color-coded) represent the desert dust source. For Fig. 3e, the concentrations in the wind speed-direction bins/cells were multiplied by frequency of occurrence and represent the dominant sources of PM_{10} over the

Table 2
Summary statistics (mean ± sd) of PM_{10}, Dust-AOD and meteorological variables for the study period 2006–2017 in AM, FKL, and BS stations. (All: all days, NDDS: Non-Desert Dust Storm days, DDS: Desert Dust Storm days).

Variable	AM			FKL			BS		
	All (n = 4383)	NDDS (n = 3573)	DDS (n = 810)	All (n = 4383)	NDDS (n = 3932)	DDS (n = 451)	All (n = 4383)	NDDS (n = 3750)	DDS (n = 633)
PM_{10} (μg/m^3)	25.9 ± 32.7	18.5 ± 7.2[i]	58.5 ± 65.0[i]	21.4 ± 24.7	17.0 ± 6.9[i]	62.9 ± 63.0[i]	55.5 ± 98.0	37.8 ± 14.2[i]	156.1 ± 226.1[i]
Dust-AOD	0.06 ± 0.10	0.03 ± 0.06[i]	0.16 ± 0.15[i]	0.06 ± 0.11	0.04 ± 0.07[i]	0.27 ± 0.17[i]	0.08 ± 0.10	0.05 ± 0.06[i]	0.21 ± 0.16[i]
Temp (°C)	19.8 ± 7.1	19.1 ± 7.2[i]	22.6 ± 6.1[i]	18.2 ± 5.6	17.9 ± 5.6[i]	20.9 ± 5.3[i]	20.0 ± 5.8	19.9 ± 5.8	20.3 ± 5.5
RH (%)	53.9 ± 14.7	54.3 ± 14.6[i]	52.4 ± 15.1[i]	71.6 ± 16.5	72.9 ± 15.5[i]	59.3 ± 20.0[i]	62.2 ± 14.6	64.0 ± 13.0[i]	51.1 ± 18.1[i]
WS (m/s)	2.9 ± 1.0	2.9 ± 1.0[i]	3.0 ± 1.3[i]	6.1 ± 3.0	6.1 ± 3.0[i]	5.7 ± 3.5[i]	2.6 ± 0.9	2.5 ± 0.8[i]	3.3 ± 1.3[i]

[i] p-Value of *t*-test <0.05.

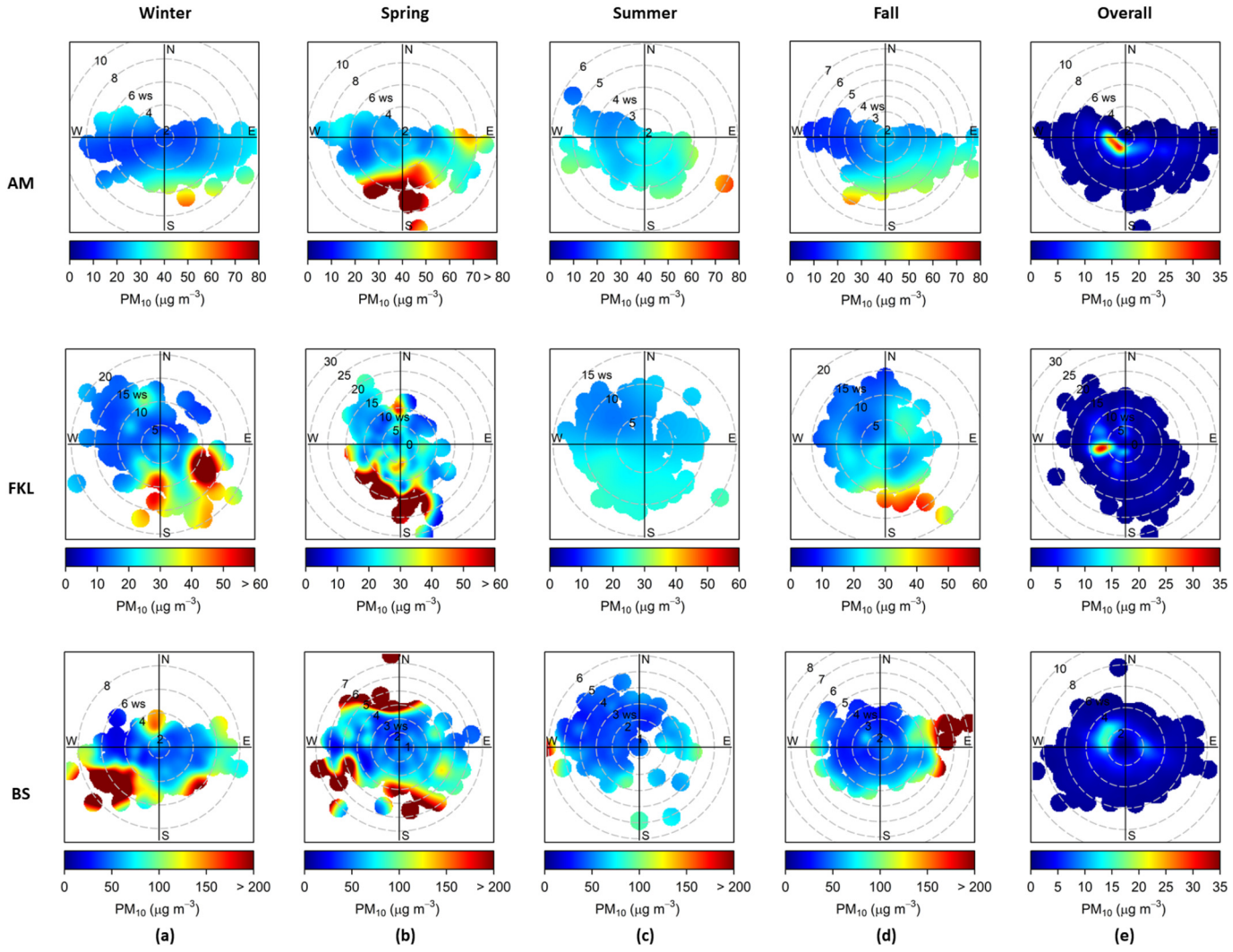

Fig. 3. Bivariate polar plots of PM_{10} concentrations (μg/m^3) per season for AM, FKL, and BS, under different seasons.

whole study period and less the DDS contribution. The weighted concentrations bivariate polar plots (Fig. 3e) show a better representation of the air mass sources that dominate the mean concentrations recorded in a previous study (Mouzourides et al., 2015).

Fig. 3a–d (AM) show that PM_{10} levels in Cyprus were strongly influenced by winds originating from S-SE regions under medium level wind speed conditions, with some seasonal variations. Specifically, South (North Africa) winds had a stronger effect in the winter and spring, SE (Arabian Peninsula) and SW (North Africa) winds had a stronger effect in the summer, and SW-S-SE (North Africa-Arabian Peninsula) winds in the fall. However, in the absence of severe DDS events (Fig. 3e-AM), the PM_{10} concentrations were mostly affected by the W-SW under very low wind speed conditions, but air masses from NE to NW were not found to be common for the island, which is in agreement with the wind climatology of the island (Jacovides et al., 2002).

FKL was highly affected by westerly winds under medium wind speed conditions (Fig. 3e-FKL). Taking into account the seasonal effect, PM_{10} sources were from south in the fall and spring, east and S-SE in the winter, and from west up to the east in the summer. FKL is highly affected by North Africa dust, especially in the summer.

In BS, the origin of PM_{10} dominant sources varied significantly by season (Fig. 3a–d). High PM_{10} levels in winter were affected by SW prevailing winds, north winds in the spring, mainly west and in some cases south and east winds in the summer; while in fall the easterly winds clearly transported high PM_{10} concentrations. During spring, the prevailing winds in the region are either west or east. However, the winds that are transporting desert dust during this season, reach the city of Beer Sheva mainly from the north, with 80% of the dust originating from the Sahara Desert. In conditions less affected by DDS events in BS (Fig. 3e-BS), we observed two prevailing conditions of PM_{10} levels; northwest winds of medium wind intensity, and secondarily the effect of eastern winds with also medium wind intensity.

3.3. Annual variability of desert dust storms characteristics

3.3.1. DDS frequency

Table 3 shows the annual incidence of DDS per site. Even though AM had the highest number of identified DDS, only 33% of them were exceeding the EU PM_{10} daily limit of 50 μg/m^3, probably due to the frequency of low intensity events or due to the fact that dust aerosol was travelling in the upper atmospheric levels above Cyprus for several of the DDS. In FKL and BS, 41% and 91% of the total DDS identified were exceeding the EU PM_{10} daily limit, respectively.

We observed a high variability in the frequency of DDS during the last decade. However, the year 2010 was the year with the highest number of DDS occurrence at all three sites. In AM, the frequency of DDS with PM_{10} exceeding the 50 μg/m^3 was also high before 2010, with a second peak in 2008. After 2010, the frequency was lower and remained relatively stable. In FKL, we observed a relatively constant number of DDS with sporadic peaks in certain years. Before 2010, the DDS above

Table 3
Annual number of DDS identified by the CART-regression combination scheme.

	2006	2007	2008	2009	2010	2011	2012	2013	2014	2015	2016	2017	Total
AM													
DDS	100	94	134	62	118	38	31	53	49	48	35	48	810
DDS with PM_{10} > 50 μg/m^3	30	34	40	18	44	11	5	20	15	17	10	21	265
Manually[a]	0	1	0	0	2	0	0	0	0	0	0	0	3
FKL													
DDS	39	46	46	27	56	35	20	51	40	31	37	23	451
DDS with PM_{10} > 50 μg/m^3	11	3	7	11	24	10	9	24	14	11	12	4	140
Manually[a]	13	36	19	5	2	4	4	2	3	6	12	6	112
BS													
DDS	54	57	49	60	83	53	45	61	37	46	47	41	633
DDS with PM_{10} > 50 μg/m^3	40	48	39	54	67	22	30	55	23	37	43	35	493
Manually[a]	15	2	0	1	0	31	15	7	9	3	6	4	93

[a] Days with missing data of PM_{10} or other variables of the rules were examined based on Dust-AOD, and satellite images.

50 μg/m^3 were only few but that is probably because of the high percentage of missing data. In BS, the frequency seems to be higher between years 2009–2013, with the exception of 2011 and 2012, for which we had ≥40% missing data for PM_{10}, and lowest in 2014. In order to identify any statistically significant linear trend of DDS frequency, we applied the Theil-Sen estimator and Mann-Kendall test of significance. The only statistically significant linear trend we found was a downtrend for AM DDS frequency (−6.2 DDS/year, p-value = 0.02), but the trend was no longer statistically significant when the analysis focused on DDS with PM_{10} daily average above 50 μg/m^3.

Previous studies in the region found an increasing trend over EM during 1958–2006 in association with changing synoptic conditions (Ganor et al., 2010), and an increasing trend on DDS frequency during 1998 and 2008 in Cyprus (Achilleos et al., 2014); but a decrease in the DDS annual number in the Mediterranean between years 2000 and 2007 (Gkikas et al., 2013), during 2001–2015 (Krasnov et al., 2016a) in Israel, and between 2003 and 2014 in the north – central area of the Iberian Peninsula (Cachorro et al., 2016).

The seasonal incidence of DDS in percentage of days per year is shown in Fig. 4. There is a significant seasonal variation of DDS across the years. Spring is the high dust season for all sites (AM: 22–54%, FKL: 29–60%, BS: 27–61%). In AM, ~50% of DDS in 2011, 2012 and 2016 occurred during spring. However, in years before 2009, 35–40% of DDS occurred in the summer (sen's slope$_{summer}$ = −3, p-value =

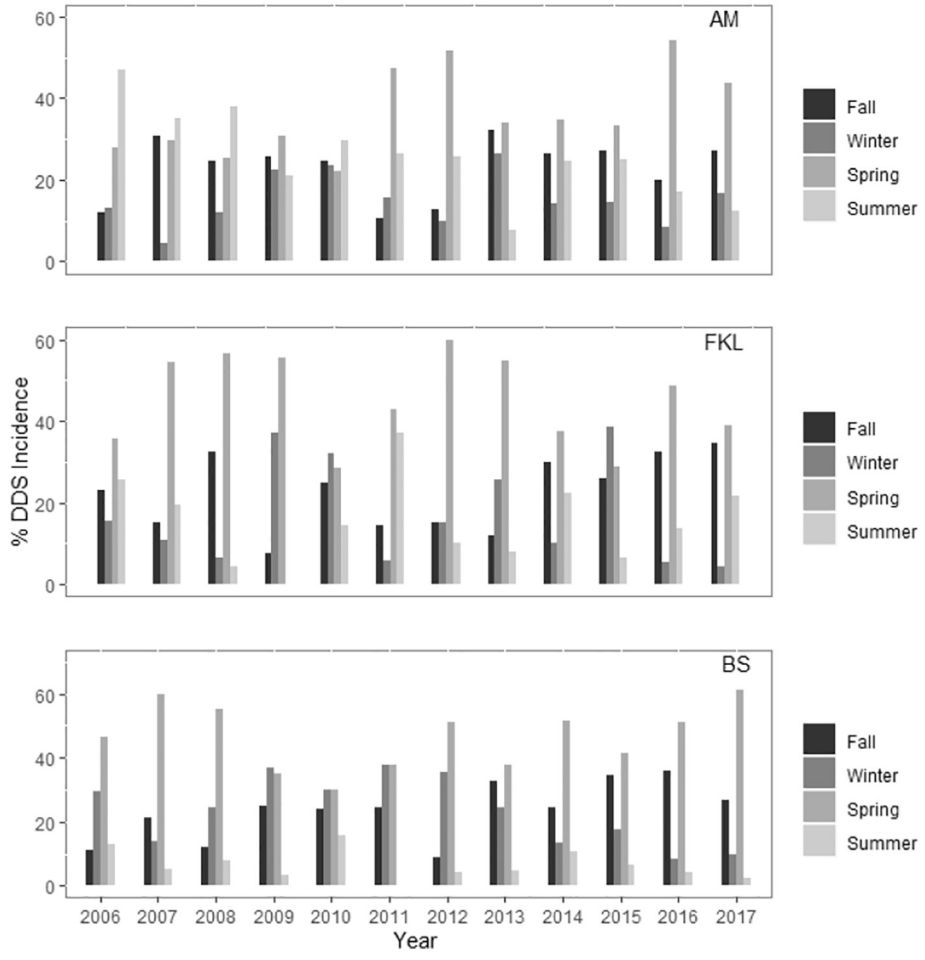

Fig. 4. Annual incidence of DDS (%) per season and year at the three sites.

0.007). In FKL, DDS were observed more often in the fall (~30% of DDS) over the last four consecutive years, 2014–2017. However, no statistically significant seasonal trend was found. In BS, there were also more DDS during fall (24–36%) for the last five years 2013–2017, but less during the winter (9–17%) over 2014–2017 (sen's $slope_{winter} = -1.2$, p-value = 0.04). A previous analysis for Israel during 1958–2006 (Ganor et al., 2010) and 2001–2015 (Krasnov et al., 2016a) years, found an increase in winter dust events.

3.3.2. DDS intensity

Even though 2010 was the year with the highest number of DDS in the region, this was not also the year with the strongest events. In AM, the annual median DDS-PM_{10} concentration levels were ~40 μg/m^3, with a maximum value in 2010 (45.3 μg/m^3) (Fig. 5). However, in 2008 and 2010 there were more DDS acting as 'outliers' in the annual DDS distribution (~>100 μg/m^3), and the maximum 24-hr DDS-PM_{10} average of 1254.6 μg/m^3 was observed during a Saharan dust episode in 2006 (25/2/2006, hourly-PM_{10}: 31.4–3540.1 μg/m^3). The Dust-AOD annual median values ranged from 0.07 (year 2006) to 0.21 (year 2016). The highest Dust-AOD values were observed in 2007 and 2012, with a 24-hr maximum in 2012 (2/5/2012, 24-hr Dust-AOD: 1.28).

In FKL, the annual median DDS-PM_{10} concentrations were between 40.7 (year 2014) and 55.8 (year 2012) μg/m^3. The year with most high intensity events were observed in 2010, and the maximum 24-hr PM_{10} average of 705.7 μg/m^3 in 2006 (24/2/2006, hourly-PM_{10}: 22.0–2717.0 μg/m^3), which corresponds to the same Saharan dust episode that AM experienced. The highest Dust-AOD values for FKL were observed in 2009, 2010 and 2015, with a 24-hr maximum in 2010 (8/3/2010, 24-hr Dust-AOD: 1.15).

In BS, PM_{10} annual median levels during DDS varied between 80.3 (year 2017) and 137.4 (year 2012-year with 69% missing data) μg/m^3. In 2009, a year with satisfactory availability of data, median DDS-PM_{10} was 112.0 μg/m^3. The years 2010 and 2015 experienced the most frequent intense events. The most extreme event was not observed in 2006, as it was in the case of AM and FKL, even BS was influenced by that dust event (26/2/2006, 24 h PM_{10}: 425.6 μg/m^3). The maximum daily PM_{10} concentration for BS was observed in 2010 with a 24-hr average of 3210.9 μg/m^3 (12/12/2010, hourly-PM_{10}: 1763–4907.0) during a three-day Saharan dust episode. The hourly PM_{10} concentration though reached the maximum (5197.8 μg/m^3) in 2012 (29/2/2012) during an ~8-hour dust episode. Dust-AOD ranged from 0.09 in 2012 to 0.23 in 2015, with the highest daily Dust-AOD average value in 2012 (2/5/201 2, 24-hr Dust-AOD: 1.28). On overall, it seems that for BS, 2010 was the year with the most frequent and most intense dust episodes. On the same time, it was the driest year of the decade with total annual precipitation of 3.7 mm (3.7 mm in 2010–245.1 mm in 2015).

Time series analysis of DDS intensity (PM_{10}, Dust-AOD) revealed that the trend is not linear. Fig. 6 shows the deviation from the PM_{10} and Dust-AOD daily mean over time (calendar date of DDS). We observed a non-monotonic trend over time. In AM, DDS-PM_{10} levels were above the average early in 2006, probably due to the most severe event of the decade, reaching a minimum during late 2006 to early 2007 and following a relatively stable PM_{10} trend afterwards with some smaller sporadic peaks. A similar pattern was observed for FKL station. Dust-AOD followed a different pattern than the one of PM_{10}, at both stations. In AM, Dust-AOD seemed to be increasing from 2009 until 2013 when it reaches a plateau. Dust-AOD in FKL follows a high variability with a big drop in years 2011 to 2012. In BS, PM_{10} levels seemed to increase from 2008 through 2010, and decreased after that with a second smaller peak in 2015. In 2015, a peak for Dust-AOD was also observed. Similar patterns were observed for hourly PM_{10} during DDS (Fig. S4).

The findings from EM studies on dust intensity vary by location, study period, and methodology. Pey et al. (2013) found no significant trend of African dust contribution to PM_{10} over central and southern Mediterranean areas (including Greece, and Cyprus) from 2001 to 2011, with sporadic annual peaks. A decreasing trend on PM_{10} contribution was observed from 2006 or 2007 through 2011 in western and central Mediterranean areas. Krasnov et al. (2016a), examined DDS events

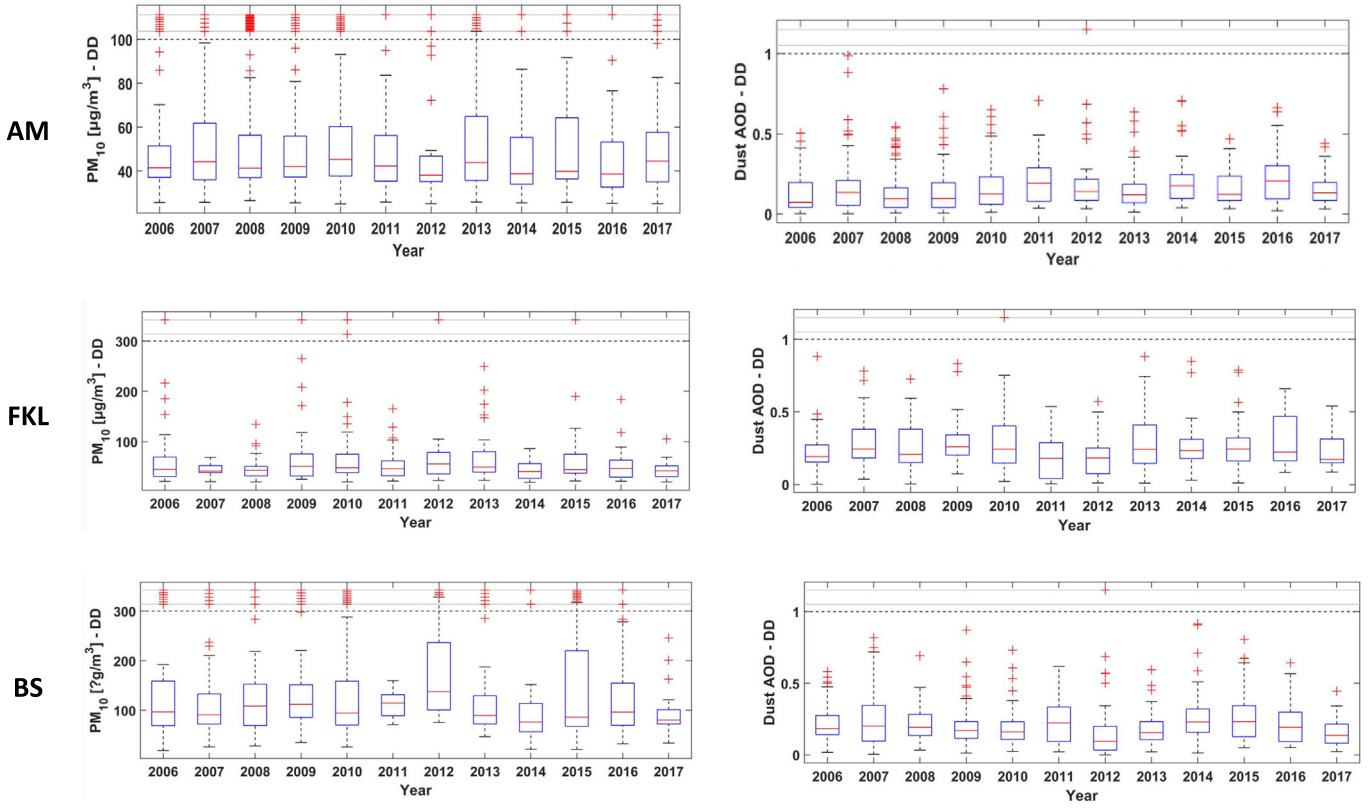

Fig. 5. Boxplots of PM_{10} concentrations (μg/m^3) and Dust-AOD during DDS per year for AM, FKL, and BS.

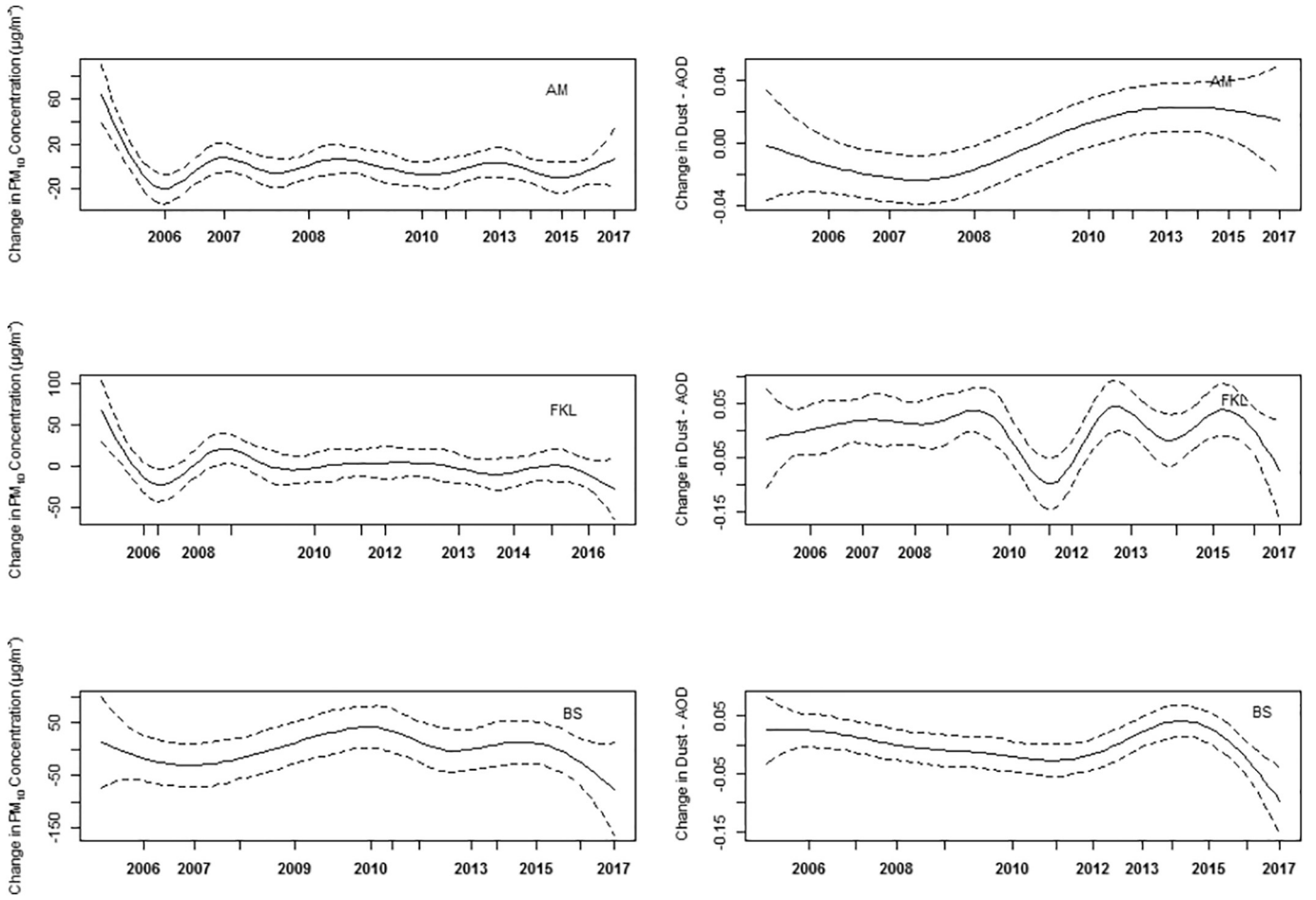

Fig. 6. Time trends of DDS-PM_{10} and DDS-DustAOD for AM, FKL, and BS station. (Dashed lines represent the 95% confidence intervals for the estimate, and marks on x-axis represent the end of the year).

in three cities in Israel for the year period 2001–2015, and found that since 2009 DDS events became more severe. We did not identify the same pattern in our analyses. This is probably due to the fact that the period of investigation is from 2006 onwards as well as the fact that a different statistical approach was adopted. Evan et al. (2016) showed that surface wind patterns are responsible for the variation of North Africa dust emissions. A historic re-analysis from 1851 to 2011, from the same authors, gave a statistically significant downtrend in the dust emissions associated with an increase in greenhouse gas emissions. In West Africa Sahel, an increase of dust emissions was observed over the last decades starting from late 1940s and it was related to droughts and to the increase in the threshold wind velocity for dust entrainment (Goudie, 2014). Model projections suggest an increase in DDS events intensity (Lelieveld et al., 2014); however, the future of DDS will depend

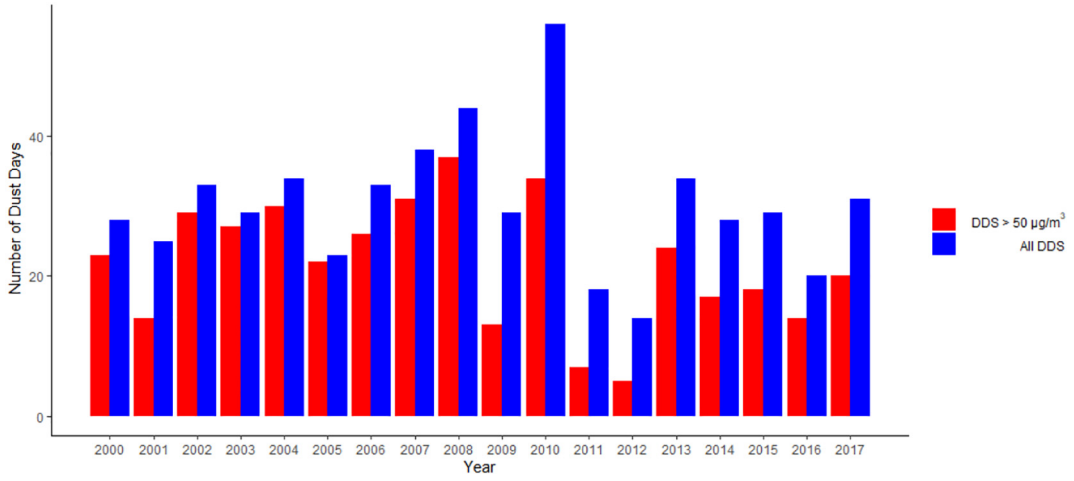

Fig. 7. Number of identified desert dust days (blue) and desert dust days with PM_{10} concentration above 50 µg/m^3 at the urban site (red) in Cyprus, per year. (For interpretation of the references to color in this figure legend, the reader is referred to the web version of this article.)

on anthropogenic pressure on desert surfaces, natural climatic variability (e.g., in the El Niño Southern Oscillation or the North Atlantic Oscillation), and climate change (Goudie, 2014).

3.3.3. DDS trend over the last two-decades (2000–2017)

Ground PM_{10} data from Cyprus are available since 1998 and they were previously used to study PM levels and DDS trends in Cyprus for the period 1998–2008 (Achilleos et al., 2014). We therefore, expanded our trends analysis and examine the DDS incidence over the last 20 years for Cyprus. However, Dust-AOD is available from year 2004 and onwards, and therefore, we were not able to use it for this analysis. In order to ensure that DDS were identified in the same way for all the years, we used the same tools from the previous analysis. We first identified suspected days of high particle levels based on: i) the 95th percentile of PM_{10} data from Nicosia urban ($PM_{10} > 87$ μg/m^3) and Ayia-Marina Xyliatos background ($PM_{10} > 57$ μg/m^3) station, and; ii) the combination of high AOD (>0.3) and low Angstrom exponent (<0.9) that signifies high load of coarse particles in the air (Barnaba and Gobbi, 2004; Gkikas et al., 2013). The AOD and Angstrom exponent data were obtained from MODIS (Moderate Resolution Imaging Spectroradiometer) TERRA Deep Blue platform at a spatial resolution of 1° × 1° (~110 km × 110 km), available since 2000. The data were downloaded from the Giovanni online data system, developed and maintained by the NASA GES DISC (https://giovanni.gsfc.nasa.gov/giovanni/). DDS were then confirmed from HYSPLIT back-trajectories (Stein et al., 2015; Rolph et al., 2017), and satellite images from NASA Worldview. This methodology was applied to Cyprus data for the period 2000, the year which satellite data started to be available, through 2017.

We identified 546 DDS in Cyprus during 2000 and 2017 years, where for more than half of events (n = 391) PM_{10} levels exceeded the daily EU limit of 50 μg/m^3 at the urban site. The annual incidence was within the small range of 20–34 DDS per year, with two peaks in 2008 (n = 44) and 2010 (n = 56), followed by two years of low incidence of DDS, in 2011 (n = 18) and 2012 (n = 14), (Fig. 7). However, even there was a significant increasing trend from 2000 to 2010 (sens' slope = 1.8, p-value = 0.04), no statistically significant trend was observed from 2000 to 2017 (sens' slope = 0, p-value = 0.88). We did not find any statistically significant trend on seasonal variability of DDS frequency and intensity (Fig. S5).

In Cyprus, the dust PM_{10} annual median ranged from 41.2 μg/m^3 (2011) to 100.6 μg/m^3 (2008) μg/m^3 at the Nicosia urban site and, from 30.1 μg/m^3 (2012) to 79.3 μg/m^3 (2008) μg/m^3 at the rural area

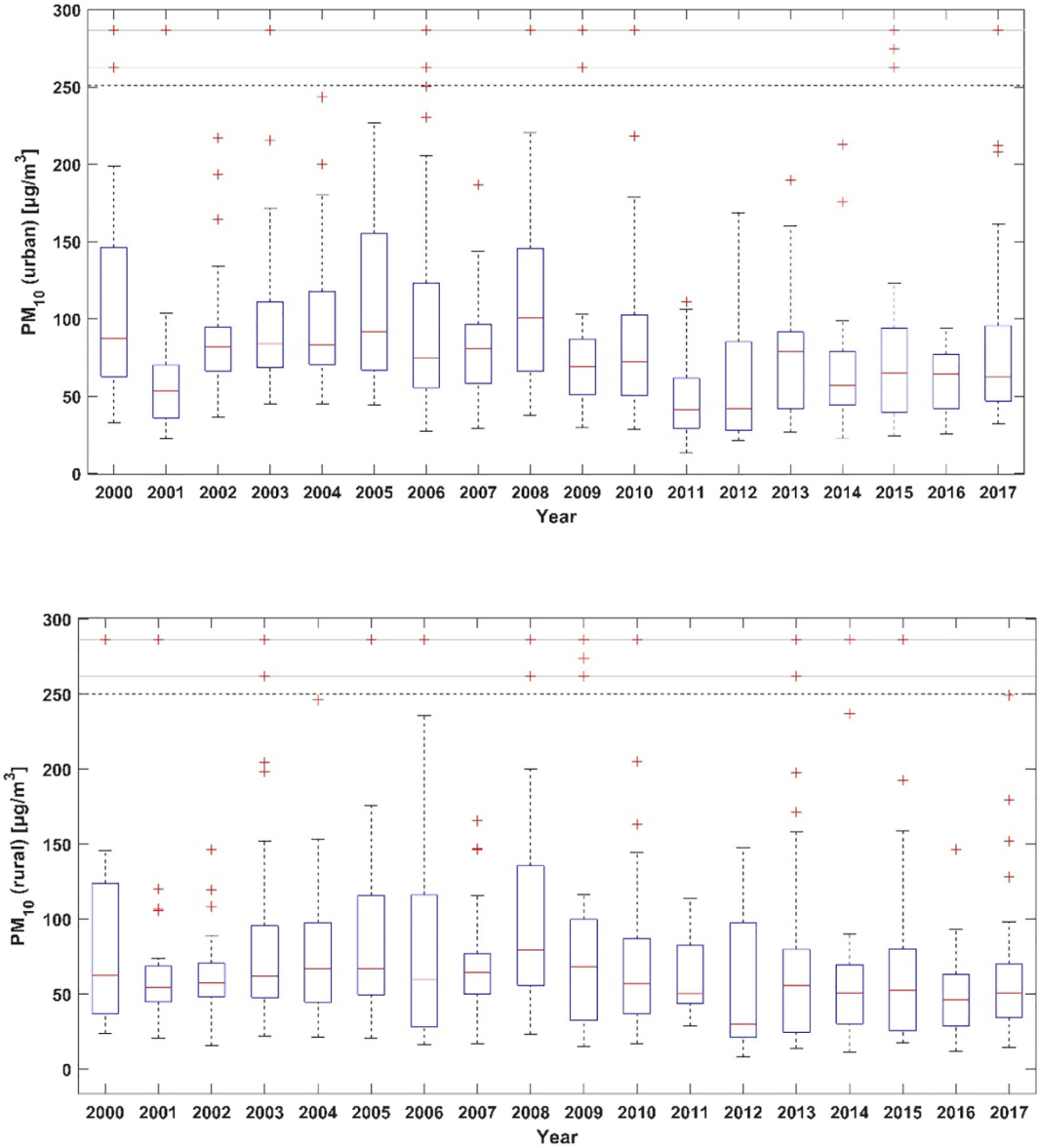

Fig. 8. Boxplots of PM_{10} concentrations (μg/m^3) during DDS at the Cyprus urban and rural areas, per year.

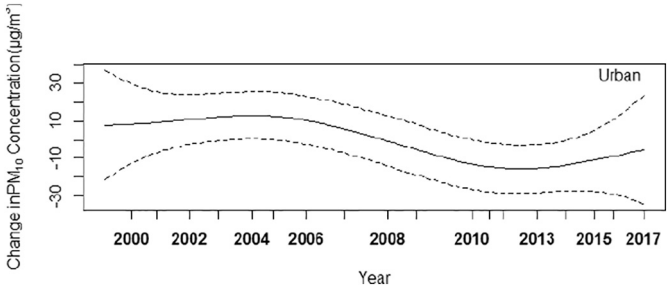

Fig. 9. Time trends of DDS-PM_{10} for Cyprus urban station. (Dashed lines represent the 95% confidence intervals for the estimate, and marks on x-axis represent the end of the year).

(Fig. 8). The highest 24-hr maximum dust PM_{10} level was observed in 2006 (urban: 1498.2 μg/m^3, rural: 1307.4 μg/m^3), and the lowest in 2016 (urban: 94.3 μg/m^3) and 2011 (rural: 113.6 μg/m^3).

During the same time, the annual total precipitation at Athalassa Meteorological Station in Nicosia ranged from 136 mm in 2008 to 437 mm in 2014 (total precipitation is calculated for calendar years). The driest year from the last 18 years was also the year with the highest frequency of DDS exceeding the EU daily limit, and highest annual DDS-PM_{10} concentration for the urban area of Nicosia.

The dust PM_{10} annual average measured at the urban and rural station in the area of Nicosia, showed a statistically significant decrease (PM_{10}urban: sen's slope = −1.7, p-value = 0.08, PM_{10}rural: sen's slope = −2.2, p-value = 0.02), but for the urban site, the decrease was not monotonic (Fig. 9). The decrease was observed during the spring season at both sites (PM_{10} urban: sen's slope = −3.5, p-value = 0.004; PM_{10}rural: sen's slope = −2.6, p-value = 0.03) (Fig. S5).

3.3.4. DDS source of origin

The influence of the two major desert dust sources of Eastern Mediterranean on the annual levels was examined from HYSPLIT trajectories (Table 4). Most of DDS originated from Saharan desert and secondly from the deserts in the Middle East (n-Saharan = 1330, n-ME = 411, n-ME-Saharan = 153). FKL is influenced almost exclusively from Saharan desert (n-Saharan = 441, n-ME = 5, n-ME-Saharan = 5) and it is therefore, not further discussed in this section. A small number of DDS was influenced by air masses originating by both Saharan and Middle Eastern deserts simultaneously. However, during years 2012 and 2015 in Cyprus and year 2013 in Israel, the number of DDS originating from ME deserts was increased. On average, DDS originating from North Africa and Middle East were of higher intensity in AM, while this was the case for episodes originating from the Saharan desert in BS.

Linear trends analysis showed that DDS originating solely from Sahara (sen's slope = −4.6, p-value = 0.02) or from both Saharan and ME deserts together (Saharan-ME) (sen's slope = −1.5, p-value = 0.008) in Cyprus, and from pure Saharan dust in Israel (sen's slope = −1.3, p-value = 0.07), decreased over years. No significant annual trend was found for their intensity (Fig. S6).

4. Conclusions

In this study, we examined DDS events in three Eastern Mediterranean areas (Cyprus, Crete-Greece, Israel) over a 12-year period, 2006 through 2017. The use of ground and columnar aerosol data made possible the identification and characterization of low and high intensity events. Days with 24-hr average PM_{10} concentration above ~30 μg/m^3 were found to be a significant indicator of DDS for the background sites of Cyprus (>35 μg/m^3) and Crete (>28 μg/m^3). Higher thresholds were found for Beer Sheva depending on the season (fall and spring: PM_{10} > 70 μg/m^3, winter and summer: PM_{10} > 90 μg/m^3).

Inter-annual variability and spatial differences were observed for different event characteristics. More frequent events were observed in Cyprus, but Israel experienced higher intensity events. All three areas were at times simultaneously affected by DDS, and this occurred for 10–20% of the DDS at each site. Israel and Cyprus had more common DDS as they are both influenced from North Africa and Arabian Peninsula deserts; Crete is rarely impacted by deserts from the East. Inter-annual variability of DDS frequency and intensity followed a relatively steady trend. The annual pattern of DDS frequency was similar for all three sites, reaching a peak in 2010. However, peaks of other DDS characteristics (PM_{10} 24 h-average, Dust-AOD, hourly and daily PM_{10} maxima, seasonality) were observed in different years, mainly due to the inter-annual variability of local, regional and global climatic conditions. In Israel and Cyprus though, the year with the highest DDS frequency and intensity was the year with the lowest precipitation. Data availability restricted our joint analysis for the three sites to the last decade only. However, analysis for Cyprus benefited from available data for 18 years. At this site, DDS frequency followed a relatively steady trend over the years, but seasonality has changed demonstrating a decrease of dust intensity during spring season.

Trend analyses for DDS characteristics differ across studies, locations and time periods. As we have seen in this work, the choice of the study period under examination can impact the results. Future studies are needed on the changes of DDS characteristics over several decades and in relation to climate change including synoptic-scale conditions.

Declaration of competing interest

The authors declare that they have no known competing financial interests or personal relationships that could have appeared to influence the work reported in this paper.

Acknowledgement

This work was supported by the European Union within the framework of the LIFE MEDEA Program under the Grant Agreement LIFE16 CCA/CY/000041.

Appendix A. Supplementary data

Supplementary data to this article can be found online at https://doi.org/10.1016/j.scitotenv.2020.136693.

Table 4
Annual number of DDS, PM_{10} (μg/m^3) and Dust-AOD levels by desert area of origin.

	2006	2007	2008	2009	2010	2011	2012	2013	2014	2015	2016	2017	Total (n)	PM_{10} (μg/m^3)	Dust-AOD
AM															
Saharan	80	56	74	42	77	30	13	23	38	22	29	28	512	58.9 ± 73.6	0.18 ± 0.15
ME	20	24	46	20	31	5	15	17	7	25	5	19	234	54.6 ± 41.9	0.13 ± 0.14
Saharan-ME	0	14	14	0	10	3	3	13	4	1	1	1	64	69.5 ± 60.0	0.19 ± 0.15
BS															
Saharan	43	32	25	39	45	33	28	24	29	29	29	21	377	170.9 ± 253.3	0.23 ± 0.16
ME	5	13	18	15	27	11	14	29	5	12	11	12	172	124.4 ± 127.4	0.19 ± 0.16
Saharan-ME	6	12	6	6	11	9	3	8	3	5	7	8	84	153.2 ± 244.4	0.20 ± 0.15

References

Achilleos, S., Evans, J.S., Yiallouros, P.K., Kleanthous, S., Schwartz, J., Koutrakis, P., 2014. PM10 concentration levels at an urban and background site in Cyprus: the impact of urban sources and dust storms. J. Air Waste Manage. Assoc. 64, 1352–1360.

Achilleos, S., Al-Ozairi, E., Alahmad, B., Garshick, E., Neophytou, A.M., Bouhamra, W., Yassin, M.F., Koutrakis, P., 2019. Acute effects of air pollution on mortality: a 17-year analysis in Kuwait. Environ. Int. 126, 476–483.

Barnaba, F., Gobbi, G.P., 2004. Aerosol seasonal variability over the Mediterranean region and relative impact of maritime, continental and Saharan dust particles over the basin from MODIS data in the year 2001. Atmos. Chem. Phys. 4, 2367–2391.

Cachorro, V.E., Burgos, M.A., Mateos, D., Toledano, C., Bennouna, Y., Torres, B., de Frutos, A.M., Herguedas, A., 2016. Inventory of African desert dust events in the north-central Iberian Peninsula in 2003–2014 based on sun-photometer-AERONET and particulate-mass-EMEP data. Atmos. Chem. Phys. 16, 8227–8248.

Chudnovsky, A.A., Koutrakis, P., Kostinski, A., Proctor, S.P., Garshick, E., 2017. Spatial and temporal variability in desert dust and anthropogenic pollution in Iraq, 1997–2010. J. Air Waste Manage. Assoc. 67, 17–26.

Diapouli, E., Manousakas, M.I., Vratolis, S., Vasilatou, V., Pateraki, S., Bairachtari, K.A., Querol, X., Amato, F., Alastuey, A., Karanasiou, A.A., Lucarelli, F., Nava, S., Calzolai, G., Gianelle, V.L., Colombi, C., Alves, C., Custodio, D., Pio, C., Spyrou, C., Kallos, G.B., Eleftheriadis, K., 2017. AIRUSE-LIFE plus: estimation of natural source contributions to urban ambient air PM10 and PM2.5 concentrations in southern Europe - implications to compliance with limit values. Atmos. Chem. Phys. 17, 3673–3685.

Ealo, M., Alastuey, A., Ripoll, A., Perez, N., Minguillon, M.C., Querol, X., Pandolfi, M., 2016. Detection of Saharan dust and biomass burning events using near-real-time intensive aerosol optical properties in the north-western Mediterranean. Atmos. Chem. Phys. 16, 12567–12586.

Evan, A.T., Flamant, C., Gaetani, M., Guichard, F., 2016. The past, present and future of African dust. Nature 531, 493.

Flores, R.M., Kaya, N., Eser, O., Saltan, S., 2017. The effect of mineral dust transport on PM10 concentrations and physical properties in Istanbul during 2007–2014. Atmos. Res. 197, 342–355.

Ganor, E., Stupp, A., Alpert, P., 2009. A method to determine the effect of mineral dust aerosols on air quality. Atmos. Environ. 43, 5463–5468.

Ganor, E., Osetinsky, I., Stupp, A., Alpert, P., 2010. Increasing trend of African dust, over 49 years, in the eastern Mediterranean. J. Geophys. Res. Atmos. 115.

Gerasopoulos, E., Kouvarakis, G., Babasakalis, P., Vrekoussis, M., Putaud, J.P., Mihalopoulos, N., 2006. Origin and variability of particulate matter (PM10) mass concentrations over the Eastern Mediterranean. Atmos. Environ. 40, 4679–4690.

Gkikas, A., Hatzianastassiou, N., Mihalopoulos, N., Katsoulis, V., Kazadzis, S., Pey, J., Querol, X., Torres, O., 2013. The regime of intense desert dust episodes in the Mediterranean based on contemporary satellite observations and ground measurements. Atmos. Chem. Phys. 13, 12135–12154.

Goudie, A.S., 2014. Desert dust and human health disorders. Environ. Int. 63, 101–113.

Inness, A., Ades, M., Agustí-Panareda, A., Barré, J., Benedictow, A., Blechschmidt, A.M., Dominguez, J.J., Engelen, R., Eskes, H., Flemming, J., Huijnen, V., Jones, L., Kipling, Z., Massart, S., Parrington, M., Peuch, V.H., Razinger, M., Remy, S., Schulz, M., Suttie, M., 2019. The CAMS reanalysis of atmospheric composition. Atmos. Chem. Phys. 19, 3515–3556.

Jacovides, C.P., Theophilou, C., Tymvios, F.S., Pashiardes, S., 2002. Wind statistics for coastal stations in Cyprus. Theor. Appl. Climatol. 72, 259–263.

Kalivitis, N., Gerasopoulos, E., Vrekoussis, M., Kouvarakis, G., Kubilay, N., Hatzianastassiou, N., Vardavas, I., Mihalopoulos, N., 2007. Dust transport over the eastern Mediterranean derived from Total Ozone Mapping Spectrometer, Aerosol Robotic Network, and surface measurements. J. Geophys. Res.-Atmos. 112.

Krasnov, H., Katra, I., Koutrakis, P., Friger, M.D., 2014. Contribution of dust storms to PM10 levels in an urban arid environment. J. Air Waste Manage. Assoc. 64, 89–94.

Krasnov, H., Katra, I., Friger, M., 2016a. Increase in dust storm related PM10 concentrations: a time series analysis of 2001–2015. Environ. Pollut. 213, 36–42.

Krasnov, H., Kloog, I., Friger, M., Katra, I., 2016b. The Spatio-Temporal Distribution of Particulate Matter during Natural Dust Episodes at an Urban Scale. PLoS ONE 11 (18). https://doi.org/10.1371/journal. pone.0160800.

Lelieveld, J., Hadjinicolaou, P., Kostopoulou, E., Giannakopoulos, C., Pozzer, A., Tanarhte, M., Tyrlis, E., 2014. Model projected heat extremes and air pollution in the eastern Mediterranean and Middle East in the twenty-first century. Reg. Environ. Chang. 14, 1937–1949.

Michaelides, S., Evripidou, P., Kallos, G., 1999. Monitoring and predicting Saharan Desert dust events in the eastern Mediterranean. Weather 54, 359–365.

Michaelides, S., Paronis, D., Retalis, A., Tymvios, F., 2017. Monitoring and forecasting air pollution levels by exploiting satellite, ground-based, and synoptic data, elaborated with regression models. Adv. Meteorol. 1–17.

Middleton, N., Yiallouros, P., Kleanthous, S., Kolokotroni, O., Schwartz, J., Dockery, D.W., Demokritou, P., Koutrakis, P., 2008. A 10-year time-series analysis of respiratory and cardiovascular morbidity in Nicosia, Cyprus: the effect of short-term changes in air pollution and dust storms. Environ. Health 7.

Mouzourides, P., Kumar, P., Neophytou, M.K.A., 2015. Assessment of long-term measurements of particulate matter and gaseous pollutants in South-East Mediterranean. Atmos. Environ. 107, 148–165.

Neophytou, A.M., Yiallouros, P., Coull, B.A., Kleanthous, S., Pavlou, P., Pashiardis, S., Dockery, D.W., Koutrakis, P., Laden, F., 2013. Particulate matter concentrations during desert dust outbreaks and daily mortality in Nicosia, Cyprus. J. Expo. Sci. Environ. Epidemiol. 23, 275–280.

Pey, J., Querol, X., Alastuey, A., Forastiere, F., Stafoggia, M., 2013. African dust outbreaks over the Mediterranean Basin during 2001–2011: PM_{10} concentrations, phenomenology and trends, and its relation with synoptic and mesoscale meteorology. Atmos. Chem. Phys. 13, 1395–1410.

Pikridas, M., Vrekoussis, M., Sciare, J., Kleanthous, S., Vasiliadou, E., Kizas, C., Savvides, C., Mihalopoulos, N., 2018. Spatial and temporal (short and long-term) variability of submicron, fine and sub-10 μm particulate matter (PM1, PM2.5, PM10) in Cyprus. Atmos. Environ. 191, 79–93.

Querol, X., Pey, J., Pandolfi, M., Alastuey, A., Cusack, M., Perez, N., Moreno, T., Viana, M., Mihalopoulos, N., Kallos, G., Kleanthous, S., 2009. African dust contributions to mean ambient PM10 mass-levels across the Mediterranean Basin. Atmos. Environ. 43, 4266–4277.

R Core Team, 2018. R: A Language and Environment for Statistical Computing. R Foundation for Statistical Computing, Vienna, Austria.

Rolph, G., Stein, A., Stunder, B., 2017. Real-time Environmental Applications and Display sYstem: READY. Environ. Model Softw. 95, 210–228.

Sorek-Hamer, M., Cohen, A., Levy, R.C., Ziv, B., Broday, D.M., 2013. Classification of dust days by satellite remotely sensed aerosol products. Int. J. Remote Sens. 34, 2672–2688.

Stein, A.F., Draxler, R.R., Rolph, G.D., Stunder, B.J.B., Cohen, M.D., Ngan, F., 2015. NOAA's HYSPLIT atmospheric transport and dispersion modeling system. Bull. Am. Meteorol. Soc. 96, 2059–2077.

Vodonos, A., Friger, M., Katra, I., Avnon, L., Krasnov, H., Koutrakis, P., Schwartz, J., Lior, O., Novack, V., 2014. The impact of desert dust exposures on hospitalizations due to exacerbation of chronic obstructive pulmonary disease. Air Qual. Atmos. Health 7, 433–439.